Characteristic time for halo current growth and rotation

Allen H. Boozer

Citation: Physics of Plasmas **22**, 102511 (2015); doi: 10.1063/1.4933363
View online: https://doi.org/10.1063/1.4933363
View Table of Contents: http://aip.scitation.org/toc/php/22/10
Published by the American Institute of Physics

Articles you may be interested in

Tokamak halo currents
Physics of Plasmas **20**, 082510 (2013); 10.1063/1.4817742

Runaway electrons and magnetic island confinement
Physics of Plasmas **23**, 082514 (2016); 10.1063/1.4960969

Theory of runaway electrons in ITER: Equations, important parameters, and implications for mitigation
Physics of Plasmas **22**, 032504 (2015); 10.1063/1.4913582

Loss of relativistic electrons when magnetic surfaces are broken
Physics of Plasmas **23**, 102513 (2016); 10.1063/1.4966046

Formation of current sheets in magnetic reconnection
Physics of Plasmas **21**, 072907 (2014); 10.1063/1.4890491

Hot tail runaway electron generation in tokamak disruptions
Physics of Plasmas **15**, 072502 (2008); 10.1063/1.2949692

PHYSICS TODAY
WHITEPAPERS

MANAGER'S GUIDE

Accelerate R&D with
Multiphysics Simulation

READ NOW

PRESENTED BY
COMSOL

Characteristic time for halo current growth and rotation

Allen H. Boozer[a)]
Department of Applied Physics and Applied Mathematics, Columbia University, New York, New York 10027, USA

(Received 30 July 2015; accepted 1 October 2015; published online 19 October 2015)

A halo current flows for part of its path through the plasma edge and for part through the chamber walls and during tokamak disruptions can be as large as tenths of the plasma current. The primary interest in halo currents is the large force that they can exert on machine components particularly if the toriodal rotation of the halo current resonates with a natural oscillation frequency of the tokamak device. Halo currents arise when required to slow down the growth of a kink that is too unstable to be stabilized by the chamber walls. The width of the current channel in the halo plasma is comparable to the amplitude of the kink, and the halo current grows linearly, not exponentially, in time. The current density in the halo is comparable to that of the main plasma body. The rocket force due to plasma flowing out of the halo and recombining on the chamber walls can cause the non-axisymmetric magnetic structure produced by the kink to rotate toroidally at a speed comparable to the halo speed of sound. Gerhardt's observations of the halo current in NSTX shot 141 687 [Nucl. Fusion **53**, 023005 (2013)] illustrate many features of the theory of halo currents and are discussed as a summary of the theory. © *2015 AIP Publishing LLC*.
[http://dx.doi.org/10.1063/1.4933363]

I. INTRODUCTION

When a plasma rapidly evolves, as during a tokamak disruption,[1–3] three types of current are important: (1) the net toroidal current flowing in the plasma, I_p, (2) the current induced in the walls or other structures surrounding the plasma, I_i, and (3) the current that flows for part of its path through the halo plasma and for part through the surrounding walls and structures, I_h. The halo plasma lies on the magnetic field lines that intercept the walls just outside the region of magnetic surfaces that confine the main plasma body.

When a plasma moves the magnetic field changes, which through Faraday's law induces voltages along both the walls and the magnetic field lines that surround the plasma. These voltages are proportional to the rate of distortion and can be balanced through Ohms law, $\vec{E} = \eta\vec{j}$ in the walls and $\vec{E}_{||} = \eta_{||}\vec{j}_{||}$ along the magnetic field lines. If a plasma were to lose force balance, the rate of plasma motion would be at an Alfvénic or sonic speed, and the currents required for an Ohmic balance would far exceed those required to restore force balance. The implication is that induced currents in the walls and halo currents arise when required to preserve plasma force balance.[4–6] An example is the resistive wall mode, which arises when in the absence of a wall the plasma would be unstable to an ideal kink mode growing on an Alvénic time scale. The induced voltages produce a current distribution in the wall that is periodic in the poloidal and the toroidal angles that slows the growth of the kink to the resistive time scale of the wall.

When the walls are too far away to stabilize a kink, a halo current arises.[4–8] The growth rate of the kink τ_k adjusts, so voltage $\mathcal{V} \equiv \int \vec{E}\cdot d\vec{\ell}$ induced along each magnetic field line, from one wall interception to the other, is consistent with the resistive voltage along that line $\mathcal{V} = \int \eta_{||} j_{||} d\ell$. The induced loop voltage along a moving magnetic field line is derived in Appendix A. The characteristic magnitude is $\mathcal{V} \sim \psi_p/\tau_k$, where ψ_p is the poloidal magnetic flux in the tokamak plasma. For ITER, $\psi_p = 100\text{V}\cdot\text{s}$, and the loss of force balance, or equivalently Alfvénic growth with $\tau_k \sim 1\mu\text{s}$, would make $\mathcal{V} \sim 10^8\text{V}$! At far lower voltages currents arise by arcing if necessary, which prevent such rapid evolution.

A commonly encountered situation in tokamaks, which results in a strong halo current, is the loss of axisymmetric positional control under plasma conditions in which the time τ_p required for the resistive decay of the plasma current is long compared to the time for the resistive decay of wall currents, τ_w. In this situation, the plasma moves axisymmetrically toward the chamber walls, which removes the outer layers of the plasma on the time scale τ_w. When $\tau_p \gg \tau_w$, the safety factor remains a fixed function of the enclosed toroidal magnetic flux, $q(\psi_t)$, on the magnetic surfaces that have not yet struck the wall. In tokamaks, reducing the toroidal flux enclosed by the plasma while holding $q(\psi_t)$ fixed implies q_{edge} drops. The drop in q_{edge} continues until a strong $n = 1$ kink arises. This occurs[9,10] when q_{edge} drops below two, but some authors[5,11] say q_{edge} drops until an $m = 1, n = 1$ kink arises. The kink near q_{edge} of two interacts too weakly with the walls for the induced currents to maintain force balance; a halo current is required. This strong halo current can be eliminated by cooling the plasma to shorten τ_p, so q_{edge} rises rather than falls as the plasma strikes the wall.

The halo current maintains force balance much as would the current in a rigid resistive shell on the plasma surface. Nevertheless, there is a major difference. The plasma halo

a)ahb17@columbia.edu

 © 2015 AIP Publishing LLC

has a negligible pressure. Unlike a rigid shell, the halo cannot sustain forces, so currents flowing through the plasma halo must flow parallel to the magnetic field lines.[4,5]

In order to maintain force balance, the halo current must produce the periodic current pattern that would arise in a rigid shell just outside the plasma. The virtual casing principle[12] implies that any plasma force-balance state requires a certain external magnetic field to sustain it. It is this external field that halo currents must produce. The constraint that the current in the plasma halo must flow along magnetic field lines implies that the required current can only be produced with limited efficiency. In particular, sidebands in the toroidal mode number n are necessarily present. This reduced efficiency is measured by a quantity $\langle \mathcal{D}^2 \rangle < 1$ defined in Ref. 7 and discussed in Section 6.3 of Ref. 8 as well as Section II of this paper.

The radial width Δ_h of the current channel in the halo plasma has a minimal width that follows from the three-legged-stool theorem. This minimal width is $\Delta_h \sim \Delta_k$, where Δ_k is the amplitude of the kinking of the tokamak plasma.

A three legged stool does not rock even when sitting on an uneven surface. More generally, when two three-dimensional objects are pushed together and at least one has no special symmetries, they will have three points of contact. An implication is that when the outermost confining magnetic surface of a kinked plasma makes contact with the chamber walls it does so only in discrete points.

The halo current extends outward radially a distance Δ_h beyond the last confining magnetic surface, which broadens the region of contact between the current channel and the walls from points to regions of finite area. In particular,[7] the toroidal extent of these areas of halo-current contact is $\Delta\varphi \approx 2\sqrt{2\Delta_h/\Delta_k}$. When $\Delta\varphi \ll 2\pi$, the halo current can enter and leave the walls in only localized regions toroidally. A theorem of Fourier analysis implies that a toroidally narrow halo current, $\Delta\varphi \ll 2\pi$, must have a broad spread of toroidal mode numbers n. This strongly couples the unstable $n=1$ kink with kinks that have $n \neq 1$, which are generally stable. It is only when Δ_h is sufficiently broad compared to the amplitude of the kink Δ_k that it becomes energetically possible for the halo current to arise.[7]

The requirement that the radial width of the current channel in the halo plasma satisfies $\Delta_h \approx \Delta_k$, the amplitude of the kink implies[7]

$$\Delta_h \approx \frac{I_h}{I_p} a \tag{1}$$

with a is the minor radius of the plasma. This follows from the result that an unstable kink held in force balance by a halo current[5,6,10] has an spatial wobble $\Delta_k \approx (I_h/I_p)a$.

The physics of the growth of the induced current of a resistive wall mode and the growth of a halo current is related. As discussed in Section II, the induced current of a resistive wall mode grows as $dI_i/dt = I_i/\tau_{rwm}$. The growth rate is $\tau_{rwm} \approx (\mu_0/\eta_w)a\Delta_w/s$, where a is the plasma minor radius, Δ_w is the thickness of the wall, and s is the stability coefficient of the kink. The radial width of the halo-current channel Δ_h increases in proportion to I_h, so the halo current grows linearly, not exponentially, in time, $dI_h/dt = I_p/\tau_g$, where $\tau_g \approx (\mu_0/\eta_w)a^2/s_{eff}$ and $s_{eff} \sim s/\langle \mathcal{D}^2 \rangle$. The non-axisymmetric halo current grows until the magnetic surfaces that confine the plasma are destroyed. Halo currents of several tenths of the original net plasma current are seen in many experiments.[1–3]

The current density in a halo current is comparable to that in the main plasma body. This follows from the relation $\Delta_h \approx (I_h/I_p)a$. The typical current density in the halo plasma $j_h = I_h/(2\pi a\Delta_h) \approx I_p/(2\pi a^2)$. Without electron emission from the walls, the current density in the halo is constrained by the ion saturation current $j_h \lesssim e n_h \sqrt{(T_e + T_i)/m_i}$, where n_h is the electron number density in the halo.[6] How this constraint affects the physics of halo currents is not well understood.

Both induced and halo currents can produce unacceptable forces in a large tokamak, such as ITER. The halo current associated with an $n=1$ kink has a strong toroidal asymmetry, which may rotate.[1,2,10,13–15] The toroidal rotation may be beneficial for spreading heat loads but could be detrimental if the rotation frequency coincides with a natural oscillation frequency of the machine structure. As will be discussed in Section III, a characteristic speed of halo current toroidal rotation is the speed of sound in the halo, $C_s = \sqrt{(T_e + T_i)/m_i}$.

Stefan Gerhardt[16] has analyzed the halo currents in NSTX. Section IV shows that the basic features of the theory of halo currents give simple interpretations of his observations: (1) When axisymmetric position control is lost, the initiation of a strong halo current occurs when q_{edge} drops to about two. (2) The amplitudes of the $n=0$ and $n=1$ components of the halo currents are comparable though both are driven by the unstable $n=1$ kink. (3) The halo current that enters the wall at a particular poloidal location is predominately of a single sign. (4) The halo current has a lobe-like structure with a full width at half maximum of about a third of the toroidal circumference and essentially independent of time. (5) A toroidal rotation of the halo current reaches approximately the halo speed of sound.

Leonid Zakharov has introduced a distinct terminology from halo currents for the currents that arise in tokamak disruptions, which can exert strong forces on the chamber walls. His terminology is discussed in Appendix B.

At present, there are few experiments to drive theory and little theory to drive experiments. The goal of this paper is to help break the impasse.

II. GROWTH OF HALO CURRENT

The expressions for the growth rates of induced and halo currents can be understood in a cylindrical model. The inductance of a thin shell in a periodic cylindrical model of a torus is $L_s = 2\pi^2 m\mu_0 R_0$, where a is the minor radius, $2\pi R_0$ is the periodicity length, and m is the poloidal mode number of the magnetic perturbation, Eq. (328) of Ref. 8. The resistance of the shell can be calculated similarly using Eq. (328) of Ref. 8, $\mathcal{R}_s = (2\pi)^2 m^2 \eta_s R_0/a\Delta_s$, where $\Delta_s \ll a$ is the thickness of the shell and η_s its resistivity. The decay time for a current in a shell

$$\frac{L_s}{R_s} = \frac{\mu_0}{\eta_s}\frac{a\Delta_s}{2m} \tag{2}$$

is independent of the length of the cylinder or equivalently the length over which the current flows.

When a rigid conducting shell is placed just outside of the surface location of a cylindrical plasma, the energy required to drive a current I_s in the shell is $L_s I_s^2/2$ when no plasma is present. The presence of plasma modifies the energy required to drive the current to $W_s = -L_s I_s^2/2s$, where a stability coefficient $s > 0$ implies instability, it takes negative energy to perturb the plasma, and $s < 0$ implies stability. The power dissipation in the shell is $\mathcal{R}_s I_s^2$. The equation $dW_s/dt = -\mathcal{R}_s I_s^2$ implies

$$\frac{L_s}{sR_s}\frac{dI_s}{dt} = I_s, \tag{3}$$

which is the equation[17] for a resistive wall mode with I_s the induced current in the shell I_i. The induced current in a resistive wall mode increases at an exponential rate $I_i \propto \exp(t/\tau_{rwm})$. Equations (2) and (3) imply

$$\tau_{rwm} = \frac{1}{s}\frac{\mu_0}{\eta_s}\frac{a\Delta_s}{2m}. \tag{4}$$

Many do not find the energy required to perturb a plasma by a particular surface current, $\delta W = -(L_s/s)I_s^2$, and the stability coefficient s intuitively obvious. The purpose of this paragraph is to build intuition, not rigor. Rigorous derivations are given in Ref. 8. The surface that is used to describe externally driven perturbations is infinitesimally outside of the bounding surface of the unperturbed plasma. The current I_s is the strength of the surface current in Amperes, and the flux Φ_s is the area of the surface times the normal magnetic field produced on the surface in the presence of the perturbing current I_s. The relation $\Phi_s = \Lambda_s I_s$ defines the effective inductance Λ_s of the surface, so $\delta W = \Phi_s^2/2\Lambda_s$. The energy δW of stability theory in ideal magnetohydrodynamics (MHD) is proportional to the square of the normal displacement of the plasma surface ξ, which is related to the normal magnetic field perturbation by $\delta B_\perp = \vec{B}_0 \cdot \vec{\nabla}\xi$. The implication is that δW is proportional to Φ_s^2, as expected from $\delta W = \Phi_s^2/2\Lambda_s$. The δW of ideal MHD is the external energy required to perturb a plasma. The stability coefficient s can be calculated using the ratio of the energy δW with a plasma present to the energy δW when no plasma is present for the same normal magnetic field on the surface, which means the same Φ_s. That is, $s \equiv -L_s/\Lambda$, where L_s is the inductance that gives δW in the absence of a plasma. The minus sign is used, since the interest is often unstable perturbations, which means negative δW. As a plasma goes from just stable to just unstable, s goes from a small negative, $|s| \ll 1$, to a small positive value. The larger s the more unstable is the plasma. Without a plasma $s = -1$, and when a plasma behaves as a rigid perfect conductor $s \to -\infty$. The external current required to produce a given normal field, $I_s = \Phi_s/\Lambda_s$, goes through zero as a plasma passes through marginal stability, $I_s = -s\Phi_s/L_s$. This is analogous to finding the force required to hold a ball in force balance when it is displaced a given distance from the top or the bottom of a hill. At the bottom of a hill, a positive force is required for a positive displacement, and the steeper the hill the more force is required. At the top of a hill, a negative force is required for a positive displacement, and the steeper the hill the more force is required to hold the ball in force balance. When the axisymmetric plasma equilibrium is known, the perturbed equilibrium code IPEC[18] can determine s.

The derivation of the equation for time evolution of the halo current requires two changes: (1) The thickness of the current channel is $\Delta_h \approx (I_h/I_p)a$. (2) The current that interacts with the unstable kink is only a fraction $\mathcal{D}$ of the halo current I_h; the remaining fraction drives stable perturbations. The energy required to drive a halo current is

$$W_s = \left(\frac{1-\langle\mathcal{D}^2\rangle}{|s_s|} - \frac{\langle\mathcal{D}^2\rangle}{s_u}\right)\frac{L_s I_h^2}{2} = -\frac{L_s I_h^2}{2s_{eff}}, \tag{5}$$

where $s_u > 0$ is the stability coefficient of the unstable kink and $s_s < 0$ is the effective stability coefficient of the stable kinks driven by the halo current. Equation (5) defines the effective stability coefficient for the halo, s_{eff}. Energy is released only when $\langle\mathcal{D}^2\rangle/(1-\langle\mathcal{D}^2\rangle) > s_u/|s_s|$, which is required for a halo current to arise and slow the growth of the unstable kink. The growth of the halo current is, therefore,

$$\frac{dI_h}{dt} = \frac{s_{eff}\mathcal{R}_s}{L_s} I_h, \tag{6}$$

$$= \frac{I_p}{\tau_g}, \text{ where} \tag{7}$$

$$\tau_g \approx \frac{1}{s_{eff}}\frac{\mu_0}{\eta_h}\frac{a^2}{2m}, \tag{8}$$

$$\frac{\mu_0}{\eta_h} \approx \frac{1.8 T_e^{3/2}\text{ms}}{(\text{eV})^{3/2}\text{meters}^2}. \tag{9}$$

In a cylindrical model, the unstable kink would often have the poloidal mode number $m = 2$.

The halo current requires a number of toroidal transits to go from one wall interception of a magnetic field line to the other.[7] The increased length of the current path increases L_s and R_s but not their ratio. The large L_s produced by the long current channel in the halo plasma implies the inductance of the return current path through the walls is generally negligible as is the resistivity of the return path.

The amplitude of the halo current ramps up linearly in time, $I_h \propto t/\tau_g$, not exponentially, where $\tau_g \approx 9\text{ms}/s_{eff}$ in NSTX under the assumptions $T_e = 10\,\text{eV}$, $a = 0.4\,\text{m}$, and $m = 2$. The actual time in NSTX observations[16] was $\tau_g \approx 15\text{ms}$ assuming $I_h = 0.2 I_p$ after 3 ms of growth. Agreement is obtained for $s_{eff} \approx 0.6$, which is not an unreasonable value.

III. HALO CURRENT ROTATION

This section will consider two mechanisms for halo current rotation. The first is the rocket effect, Section III A,

which derives from momentum conservation together with the flow of mass out of the opposite ends of a magnetic flux tube where it contacts the wall. This effect scales with the speed of sound in the halo plasma or equivalently with the square root of the temperature in the halo plasma. The second is the radial electric field effect, Sec. III B, which derives from the radial electric field required for quasi-neutrality. This effect scales linearly with the temperature of the halo plasma.

A. Rocket effect

When the loss of plasma is not equal at the two interception points of an open magnetic field line with the wall, there will be an unbalanced rocket-effect force. The rocket force is well known from toy balloons. When the nozzle of a balloon is held closed, the pressure force balances over the interior surface of the balloon; the pressure exerts no net force. When the nozzle is open, the pressure force is missing in the region of the nozzle, so the pressure exerts a net force in the opposite direction to the nozzle. In a rocket, a force arises if the flow channel varies in cross-sectional area even when the channel is smooth.

The rocket force can be brought into balance if the magnetic structure in which the halo plasma is embedded has a particular toroidal rotation velocity u, which is generally comparable to the speed of sound C_s in the halo. When this effect is dominant, the toroidal rotational period of the halo currents is

$$\tau_{rot} = \frac{2\pi R_0}{M_h C_s}, \tag{10}$$

$$= \frac{1}{M_h}\frac{6.4\text{ms}}{\sqrt{(T_e+T_i)/\text{eV}}}\frac{R_0}{\text{meters}}, \tag{11}$$

where $M_h \equiv u/C_s$ is the Mach number of the rotation. For the NSTX experiment featured in Gerhardt's paper,[16] agreement is obtained with the estimates $T_e + T_i = 20\text{eV}$ and $M_h \sim 1$ since $R_0 = 0.85\text{m}$.

Several effects could compete with the rocket-force effect on halo current rotation. (1) The central plasma could couple to the non-axisymmetric magnetic perturbation through the neoclassical toroidal viscosity (NTV) and through its inertial effect greatly slow the spin up of the magnetic structure.[13] If the NTV effect is assumed to be dominant, as assumed in Ref. 13, the rotation would be at a diamagnetic rate. (2) The halo plasma could have a non-ambipolar flow along the open magnetic lines of the halo plasma with the associated currents closing in the chamber walls.[13] Section III B shows the natural rotation speed of the magnetic structure is E_r/B_θ. (3) If the resistive time constant of the wall τ_w times the rotation frequency of the halo currents were of order unity, the wall would exert a strong drag. But when halo currents rotate, the rotation rate is much larger, which makes the resistive-wall force small. (4) Non-axisymmetries in the walls or the external magnetic field could lock the magnetic asymmetry in a particular toroidal position until the rocket force reaches a certain level.

1. Basic equations

The velocity moment of the Fokker-Planck equations for the ions and electrons implies that

$$\frac{\partial \rho\vec{v}}{\partial t} + \vec{\nabla}\cdot\left(\rho\vec{v}\vec{v} + \overleftrightarrow{p}\right) = \vec{j}\times\vec{B}. \tag{12}$$

For simplicity, one can assume $\overleftrightarrow{p} = p\overleftrightarrow{1}$, which implies viscous forces are ignored, and the properties of steady-state solutions can be studied. Equation (12) can then be written as

$$\vec{\Gamma}\cdot\vec{\nabla}\frac{\vec{\Gamma}}{\rho} + \vec{\nabla}p + \vec{\Gamma}\frac{s_\rho}{\rho} = \vec{j}\times\vec{B}, \tag{13}$$

where the mass flux $\vec{\Gamma} \equiv \rho\vec{v}$ obeys the continuity equation, $\vec{\nabla}\cdot\vec{\Gamma} = s_\rho$. The mass source s_ρ is assumed to add particles but not momentum. The continuity equation follows from the integration of the ion kinetic equation over velocity space.

In the halo, the flow is essentially parallel to the magnetic field, so one can use the approximation $\vec{\Gamma} = (\Gamma/B)\vec{B}$. The continuity equation becomes

$$\vec{B}\cdot\vec{\nabla}\frac{\Gamma}{B} = s_\rho. \tag{14}$$

The simplest reference frame for the plasma calculation is the one in which the magnetic-field structure is stationary. The toroidal rotation of the field structure relative to the walls at a velocity u can be incorporated by adding a velocity $u_{||} = uB_\varphi/B$ to the parallel velocity of the plasma where it intercepts the walls. In the frame in which the magnetic field is stationary $\vec{B}\cdot\vec{\nabla} = B\partial/\partial\ell$, where ℓ is the distance along a magnetic field line or better the distance along a magnetic flux tube. The cross-sectional area of a tube that contains a fixed magnetic flux $\delta\psi$ is $\delta A = \delta\psi/B$. The variation in the cross-sectional area of the flow channel, which has a fundamental role in the theory of rockets, is replaced by the variation in the magnetic field strength with ℓ in the theory of halo rotation.

Equation (14) has the form

$$\frac{\partial}{\partial\ell}\frac{\Gamma}{B} = \frac{s_\rho}{B}. \tag{15}$$

The mass flux divided by the magnetic field strength at the point where the field line exits the wall $(\Gamma/B)_{ex}$ and where it enters $(\Gamma/B)_{en}$ is

$$\left(\frac{\Gamma}{B}\right)_{en} - \left(\frac{\Gamma}{B}\right)_{ex} = \sigma_{tot}, \text{ where} \tag{16}$$

$$\sigma_{tot} \equiv \int_{en}^{ex}\frac{s_\rho}{B}d\ell. \tag{17}$$

The total source of mass in a small tube carrying a magnetic flux $\delta\psi$ along the field line is $\sigma_{tot}\delta\psi$; the volume of the flux tube is $\delta V = \delta\psi\int_{ex}^{en} d\ell/B$.

Force balance along the magnetic field becomes

$$\Gamma\frac{d\Gamma/\rho}{d\ell} + \frac{dp}{d\ell} + \Gamma\frac{s_\rho}{\rho} = 0. \tag{18}$$

2. Analytic solution

Given the mass source $s_\rho(\ell)$, the speed of sound $C_s(\ell) \equiv \sqrt{dp/d\rho}$, and the magnetic field strength $B(\ell)$ along a magnetic field line, Eqs. (15) and (18) can be solved. Nonetheless, finding solutions is subtle because of the role of sonic points, and analytic results clarify the nature of solutions.

To obtain an analytic solution, it will be assumed that the mass source is in a region of constant magnetic field strength B_c and density ρ_c with the maxima of the field strength in the two directions along the line B^m_{en} and B^m_{ex} significantly greater than B_c, an assumption required to make the density constant in the region of the source. The temperature is assumed constant along the magnetic field lines so $p = \rho C_s^2$, where

$$C_s \equiv \sqrt{\frac{T_e + T_i}{m_i}} \tag{19}$$

is a constant.

Outside of the region of the mass source, Eq. (18) can be written using the density as the independent variable as

$$\frac{d\Gamma^2}{d\rho} = -2\rho\left(C_s^2 - \frac{\Gamma^2}{\rho^2}\right). \tag{20}$$

Equation (20) is well known in fluid mechanics from the theory of nozzles and says the density drops as the flux Γ increases until the flux achieves its maximum possible value where $v_{||}^2 = (\Gamma/\rho)^2 = C_s^2$.

The solution of Eq. (20) for the parallel flux and the parallel velocity is

$$\Gamma^2 = \rho^2 C_s^2\left(M_c^2 + \ln\left(\frac{\rho_c}{\rho}\right)^2\right), \tag{21}$$

$$\frac{v_{||}^2}{C_s^2} = M_c^2 + \ln\left(\frac{\rho_0}{\rho}\right)^2, \tag{22}$$

where ρ_c and M_c^2 are constants; M_c is the Mach number of the parallel flow at the density ρ_c. The Mach number M_c is generally different on the two sides of the source region, the sides on which magnetic field lines exit and enter the surrounding wall.

Equation (20) can be used to obtain a Taylor expansion of Γ^2 about ρ_m, the density at the magnetic field maximum, where $d\Gamma^2/d\rho = 0$. Since $d^2\Gamma^2/d\rho^2 = -2(C_s^2 + \Gamma^2/\rho^2)$,

$$\Gamma^2 = \Gamma_m^2\left(1 - 2\frac{(\delta\rho)^2}{\rho_m^2}\right), \tag{23}$$

where $\delta\rho \equiv \rho - \rho_m$, which is positive in subsonic and negative in supersonic flow. Since Γ/B is constant

$$\frac{(\delta\rho)^2}{\rho_m^2} = \frac{1}{2}\left(1 - \frac{B^2}{B_m^2}\right) = \frac{B_m - B}{B_m} \equiv \frac{\delta B}{B_m} \text{ as } \delta B \to 0. \tag{24}$$

The mass flux of the two field maxima must equal the source $(\Gamma^m_{ex}/B^m_{ex}) - (\Gamma^m_{en}/B^m_{en}) = s_{tot}$, which determines ρ_c. Beyond the magnetic field maximum, the flow becomes supersonic.

The net force exerted on the plasma at the entry or exit point of magnetic flux tube from the wall is given by $(\rho(v_{||} + u_{||})^2 + p)/B$, where $u_{||} = \hat{b}\cdot\vec{u}$ is the velocity of the magnetic structure relative to the walls—the basic calculation of the plasma flow was made in the frame in which the magnetic structure was stationary. Since $p = \rho C_s^2$, this force can also be written as $\rho((v_{||} + u_{||})^2 + C_s^2)/B$.

In steady state, the net force on the magnetic structure is in balance though the force does not balance flux tube by flux tube since the magnetic field forms an essentially rigid structure. As in a rocket, the change in the cross-sectional area of the tube in which the flow takes places allows net pressure forces exerted perpendicular to the tube to accelerate it. Even the dynamic pressure force, $\vec{\nabla}\cdot(\rho v_{||}^2\hat{b}\hat{b})$ contributes, where $\hat{b} \equiv \vec{B}/|\vec{B}|$. This force is $\rho v_{||}\hat{b}\cdot\vec{\nabla}(v_{||}\hat{b}) = (\Gamma\hat{b}\cdot\vec{\nabla}(\Gamma/\rho))\hat{b} + \rho v_{||}^2\vec{\kappa}$. The curvature of the magnetic field lines, $\vec{\kappa} = \hat{b}\cdot\vec{\nabla}\hat{b}$, is perpendicular to the magnetic field but has a component in the toroidal direction.

The determination of $u_{||}$ from force balance for the magnetic structure requires an integral over the magnetic flux at exit and entry to the wall. In some sense, the net force must balance on the typical magnetic flux tube,

$$\left(\frac{\rho\left((|v_{||}| - u_{||})^2 + C_s^2\right)}{B}\right)_{ex} = \left(\frac{\rho\left((v_{||} + u_{||})^2 + C_s^2\right)}{B}\right)_{en}, \tag{25}$$

which determines the velocity $u_{||}$ of the magnetic field structure.

A simple force-balance calculation arises when the field maxima are on the walls, then

$$\frac{u_{||}}{C_s} \approx \frac{1}{2}\frac{\dfrac{\rho^m_{ex}}{B^m_{ex}} - \dfrac{\rho^m_{en}}{B^m_{en}}}{\dfrac{\rho^m_{ex}}{B^m_{ex}} + \dfrac{\rho^m_{en}}{B^m_{en}}}. \tag{26}$$

The above equation and Eq. (24) imply the toroidal Mach number of the magnetic structure is

$$\frac{u_{||}}{C_s} \approx \frac{1}{4}\left(\sqrt{\frac{\delta B_{ex}}{B_m}} - \sqrt{\frac{\delta B_{en}}{B_m}}\right). \tag{27}$$

The flux of momentum, $\mathcal{F} = \rho(v_{||}^2 + C_s^2) = (\Gamma^2/\rho) + \rho C_s^2$, can be Taylor expanded in $\delta\rho$

$$\mathcal{F} = \mathcal{F}_m\left(1 + \frac{\delta\rho^2}{2\rho_m^2}\right) + \frac{\delta\Gamma^2}{\rho_m} = \mathcal{F}_m\left(1 - \frac{\delta\rho^2}{2\rho_m^2}\right). \tag{28}$$

The force on a flux tube is given by $\mathcal{F}/B$. Equation (28) implies that as $\delta B/B_m \to 0$

$$\frac{\mathcal{F}}{B} = \left(\frac{\mathcal{F}_m}{B_m}\right)\left(1 + \frac{\delta B}{2B_m}\right), \tag{29}$$

where $\delta B \equiv B_m - B$. The momentum flux is greater when the wall is not the location of the maximum of the magnetic field strength. Nevertheless, when $\delta B/B_m \ll 1$ all along the flux tube, the evaluation of $u_{||}$ at the maxima of the magnetic field strength is an accurate approximation.

David Bohm[19] showed that to obtain a physical boundary condition for a plasma flowing onto neutralizing surface, such as a wall, the plasma flow speed into the surface must exceed $\sqrt{T_e/m_i}$. The flow is supersonic beyond the magnetic field maximum. Nonetheless, the Bohm condition $|v_{||}| - |u_{||}| \geq \sqrt{T_e/m_i}$ at the field line interception that is propelling the flow can serve as a choke on the outflow and reduce $|u_{||}|/C_s$.

B. Radial electric field effect

A radial electric field E_r produces a toroidal rotation E_r/B_θ between a non-axisymmetric magnetic structure and a plasma, where B_θ is the poloidal magnetic field.

The magnetic perturbation can be written as $\delta\vec{B}\cdot\vec{\nabla}\psi_t = S(\theta)\sin n(\varphi - \varphi_0) + C(\theta)\cos n(\varphi - \varphi_0)$, where the phase factor φ_0 rotates, $d\varphi_0/dt = v_{||}/R_0$ with $v_{||}$ the velocity along the magnetic field and R_0 the major radius. When the plasma and the magnetic structure are tightly coupled, the poloidal flow must vanish in a torus—unlike the case in a cylinder where modes of the magnetic perturbations have helical symmetry with a fixed m and n.

The natural ambipolar electric field when magnetic surfaces exist is given by $enE_r = dp/dr \approx nT/\Delta$ where Δ is the scale of the pressure gradient. The plasma flow is $\vec{v} = (-E_r/B + v_{||}r/qR_0)\hat{\theta} + (v_{||}/R)\varphi$. No poloidal flow relative to the structure requires $v_{||} = E_r/B_\theta$, where

$$v_{||} = \frac{T}{eB_\theta}\frac{1}{\Delta} = C_s\frac{\rho_\theta}{\Delta}, \tag{30}$$

where ρ_θ is the poloidal gyroradius.

End losses on open magnetic field lines are ambipolar when the electric potential $\Phi \sim 3T_e/e$, which gives a somewhat larger radial electric field, when Δ is the radial scale of the electron temperature on the open lines.

There is no requirement that the end losses be ambipolar, and currents flowing in and out along magnetic field lines that contact a wall produce a force between the plasma and even an axisymmetric wall that is perfectly conducting.[13] The ions in the plasma produce the required balancing force when the thickness of the open field line region is comparable to the radial distance that the ions that strike the walls cross the magnetic field. The non-ambipolar force is important when the safety factor times the ion gyroradius is comparable to the width of the halo current, Δ_h.

IV. SUMMARY AND EXPERIMENTAL COMPARISON

Stefan Gerhardt[16] analyzed the features of halo currents in NSTX and in particular gave a detailed description of the evolution of the halo current in shot 141 687. The theory developed in this and an earlier paper[7] can be summarized by a comparison with Gerhardt's description of the evolution of the halo current in that shot.

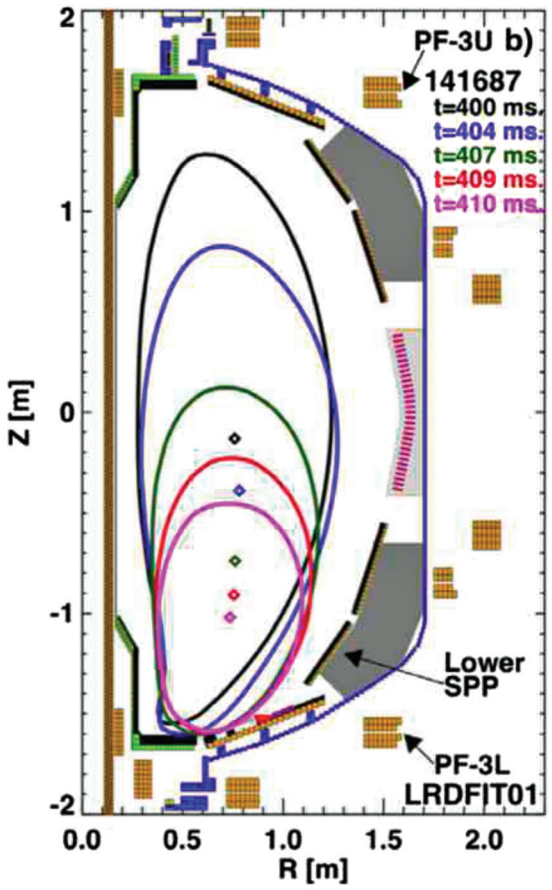

FIG. 1. Axisymmetric plasma control was lost at 400 ms in NSTX shot 141 687, and the plasma moved downward on a time scale set by the resistivity of the wall. A strong halo current was developing in the bottom-most illustrated plasma position. The halo current was measured using six instrumented tiles that were outboard from the open slot at the bottom of the plasma chamber. This figure was part of Figure 2 of Ref. 16 and is reproduced with permission from S. P. Gerhardt, Nucl. Fusion **53**, 023005 (2013). Copyright 2013 International Atomic Energy Agency.

The loss of axisymmetric control is a standard starting point for the development of a strong halo current. As illustrated in Figure 1 axisymmetric control was lost 400 ms into NSTX shot 14 687 and the plasma moved toward the divertor region at the bottom of the confinement chamber. The plasma current dropped as the plasma moved downward, Figure 2, but the plasma conductivity was sufficiently high that the edge safety factor, q_{edge}, also dropped as the outer parts of the plasma were lost by being pushed into the wall, Figure 3. A weak halo current was seen, Fig. 4, as q_{edge} passed through three at 408 ms, and a strong halo current,

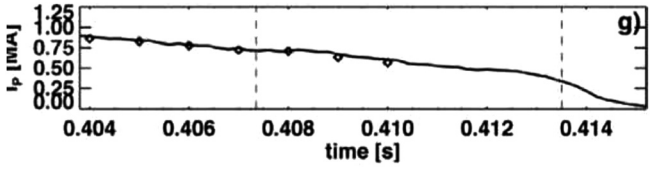

FIG. 2. Although the plasma current in NSTX shot 141 687 dropped significantly before 410 ms, the primary drop was later, during the period of a strong halo current. This figure was part of Figure 2 of Ref. 16 and is reproduced with permission from S. P. Gerhardt, Nucl. Fusion **53**, 023005 (2013). Copyright 2013 International Atomic Energy Agency.

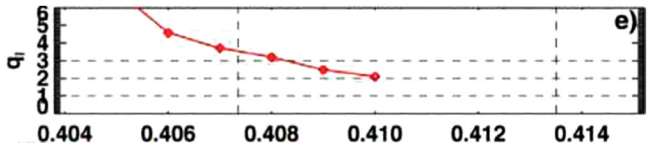

FIG. 3. At 410 ms in NSTX shot 141 687, the edge safety factor reached $q_{edge} \approx 2$, and a strong halo current arose. A weaker halo current arose when the plasma passed through $q_{edge} = 3$ at approximately 408 ms. This figure was part of Figure 2 of Ref. 16 and is reproduced with permission from S. P. Gerhardt, Nucl. Fusion **53**, 023005 (2013). Copyright 2013 International Atomic Energy Agency.

which eventually terminated the plasma, arose as q_{edge} reached two at 410 ms. The smallest and bottom-most plasma in Figure 1 is at 410 ms with $q_{edge} \approx 2$. This description of the development of a strong halo current when axisymmetric control is lost is what is expected theoretically, as discussed in the Introduction.

The halo current had striking features, Fig. 4, which are nonetheless expected theoretically. The $n = 0$ and the $n = 1$ parts of the halo current were essentially equal starting from the period with a moderate halo current when q_{edge} was approximately three at 408 ms through the period with a much stronger halo current associated with $q_{edge} \approx 2$ between 410 ms and 413.8 ms. The locking together of these two Fourier amplitudes is what is expected when the width of the halo current Δ_h is comparable to the amplitude of the kink and the coupling efficiency $\langle \mathcal{D}^2 \rangle$ is comparable to but nonetheless significantly less than unity.[7] Another theoretical finding of Ref. 7 is that the halo current at a given poloidal location is predominant of a single sign, and this striking feature was seen in NSTX shot 141 687, Fig. 4.

The correct interpretation of comparable $n = 0$ and $n = 1$ amplitudes is not that there is an axisymmetric and a non-axisymmetric drive for the halo current. Theoretically both Fourier harmonics are driven by the energy released by the unstable $n = 1$ kink, Ref. 7 and Section II. The coupling of the $n = 0$ and $n = 1$ harmonics was clear in shot 141 687, not only from the essentially identical time dependence of the $n = 0$ and $n = 1$ amplitudes, Figure 4, but also because the halo current flowed in a toroidal lobe with a full width at half maximum of about a third of the toroidal circumference,

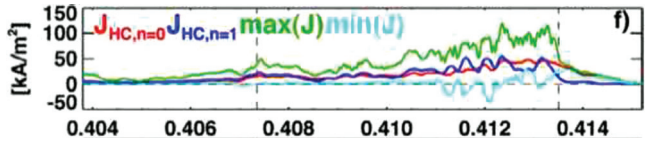

FIG. 4. The axisymmetric, $n = 0$, halo current in red and the $n = 1$ halo current in blue in NSTX shot 141 687 had essentially identical magnitudes before 413.8 ms. The halo current then became essentially axisymmetric until it disappeared at 414.4 ms. The maximum of halo current entering one of the instrumented tiles tracked the $n = 0$ and $n = 1$ halo current components as long as they tracked each other. During this period, the minimum halo current $min(J)$ entering an instrumented tile had a small amplitude though $min(J)$ could, in principle, be large in amplitude but negative. The current going into the instrumented tiles was predominately of one sign. This figure was part of Figure 2 of Ref. 16 and is reproduced with permission from S. P. Gerhardt, Nucl. Fusion **53**, 023005 (2013). Copyright 2013 International Atomic Energy Agency.

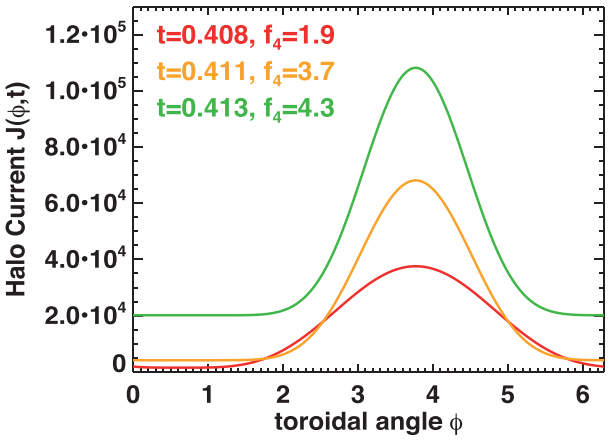

FIG. 5. During the period of a strong halo current between 408 ms and in NSTX shot 141 687, the halo current going into the instrumented tiles formed a lobe, which had a toroidal width that was essentially independent of time. The full width at half maximum of the lobe was about a third of the toroidal circumference. This figure was provided by S. Gerhardt in a private communication.[24]

Figure 5, throughout the period 410 ms to 413 ms. To obtain this result Gerhardt used the function

$$f(t,\phi) = f_0 + f_1 \cos^{2f_4}\left(\frac{\phi - f_2 - f_3 t}{2}\right), \tag{31}$$

where f_0, f_1, and f_4 are the functions of time, to fit the currents going into the instrumented tiles, which were outboard from the slot at the bottom of the plasma chamber. This fitting function not only showed the existence of a lobe of essentially constant width but also that the offset of the wings of the lobe from zero current amplitude, the function $f_0(t)$, is small, Figure 6, though rising near the end of the strong halo-current period.

The growth of the halo current appeared to be linear in time in Figures 4 and 6, which is consistent with a simple interpretation of Eq. (7), and as noted in the discussion of this equation, the halo growth time, Eq. (9), is consistent with the experimental observation for a credible stability coefficient s_{eff}. Neither the total halo current nor the halo

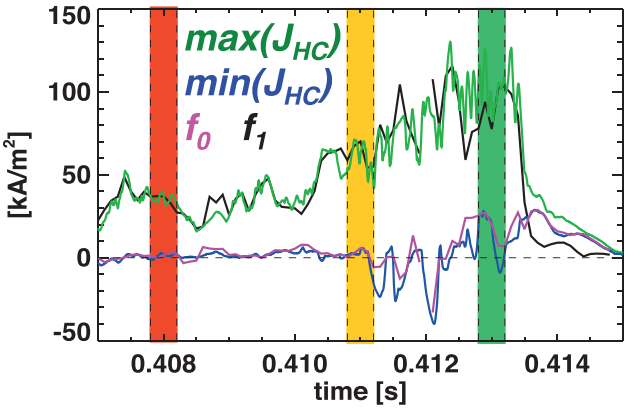

FIG. 6. Gerhardt's f_1 parameter, Eq. (31), and the maximum current going into an instrumented tracked together before 13.8 ms in NSTX shot 141 687. During the period before 13.8 ms, the offset, Gerhardt's f_0 parameter, was small as was the minimum of the halo current going into an instrumented tile. This figure was provided by S. Gerhardt in a private communication.[24]

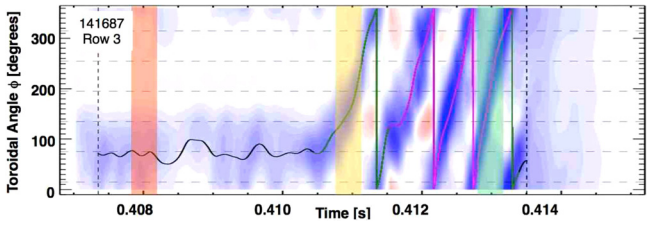

FIG. 7. The lobe of the halo current began to toroidally rotate at 410.5 ms in NSTX shot 141 687. The rotational period went from about 1 ms to about 0.6 ms before the toroidal lobe disappeared. This figure was part of Figure 2 of Ref. 16 and is reproduced with permission from S. P. Gerhardt, Nucl. Fusion **53**, 023005 (2013). Copyright 2013 International Atomic Energy Agency.

temperature was given by Gerhardt, and insufficient information is known about the main plasma for a direct calculation of s_{eff}, so this comparison is necessarily qualitative.

The lobe of the halo current was observed to rotate toroidally in NSTX shot 141 687, Fig. 7. Before 410.5 ms, the position of the lobe oscillated about a fixed toroidal location, as if trapped by a magnetic field error, but broke free when the halo current became sufficiently strong. The first rotation period was about 1 ms but the later three rotation periods were shorter, about 0.6 ms. The toroidal rotation speed is roughly sonic as expected from the rocket effect, Eq. (27). Rotational locking of ordinary kinks has the opposite tendency—free rotation at low amplitude and locking at high.

Even the symmetrization of the halo current between 413.8 ms and 414.4 ms seen in Figures 4 and 6 has a simple explanation. The time 413.8 ms is roughly when the last magnetic surfaces were lost. After that time, all of the magnetic field lines that passed through the plasma are thought to have struck the walls. The normal magnetic field to the wall, which was approximately axisymmetric before strong kinking occurred and presumably remained axisymmetric because the evolution of the kink was rapid compared to the resistive wall time. By this time, the plasma pressure was too low to balance a significant $\vec{j}\times\vec{B}$ force, so whatever current remained had to flow parallel to magnetic field lines from one axisymmetric interception with the walls to the other, which has an axisymmetric halo current as its natural solution.

ACKNOWLEDGMENTS

This material was based upon the work supported by the U.S. Department of Energy, Office of Science, Office of Fusion Energy Sciences under Award No. De-FG02-03ER54696.

APPENDIX A: VOLTAGE ALONG A MOVING MAGNETIC FIELD LINE

The voltage induced along a moving magnetic field line, $\mathcal{V}\equiv\int_{ex}^{en}\vec{E}\cdot d\ell$, between the point of wall exit to the point of wall entry is given by Faraday's Law

$$\frac{\partial\mathcal{V}(\psi_p,\varphi_0,t)}{\partial\varphi_0}=-\frac{1}{2\pi}\left[\vec{u}\cdot\vec{\nabla}\psi_p\right]_{ex}^{en}. \tag{A1}$$

The magnetic field line velocity $\vec{u}$ is defined by $\vec{E}+\vec{u}\times\vec{B}=-\vec{\nabla}\Phi$, a relation that always holds in a local spatial region.[20] The poloidal flux ψ_p and the Clebsch angle φ_0 are defined so $2\pi\vec{B}=\vec{\nabla}\psi_t\times\vec{\nabla}\theta+\vec{\nabla}\varphi\times\vec{\nabla}\psi_p=\vec{\nabla}\varphi_0\times\vec{\nabla}\psi_p$. The quantity $[\cdots]_{ex}^{en}$ is the difference between the value at the entrance and exit points. Equation (A1) can be derived by dotting the electric field with $\partial\vec{x}/\partial\varphi_0$, where $\vec{x}(\psi_p,\varphi_0,\ell)$ gives positions in Clebsch coordinates and ℓ is the distance along a magnetic field line. The derivation uses standard relations from the theory of general coordinates, which are given in the Appendix of Ref. 8. The resulting equation, $\vec{E}\cdot(\partial\vec{x}/\partial\varphi_0)-\vec{u}\cdot\vec{\nabla}\psi_p=-\partial\Phi/\partial\varphi_0$, is evaluated at the two interceptions of a field line with a perfectly conducting wall, where the tangential electric field vanishes, $\vec{E}\cdot(\partial\vec{x}/\partial\varphi_0)=0$. The voltage $\mathcal{V}\equiv\int_{ex}^{en}\vec{E}\cdot d\vec{\ell}=-[\Phi]_{ex}^{en}$. Equation (A1) then follows.

APPENDIX B: ZAKHAROV'S TERMINOLOGY

Leonid Zakharov has introduced distinct terminology for the currents that arise during tokamak disruptions, currents that can exert large forces on the walls. He speaks of Hiro and Evans currents and dismisses halo currents as being irrelevant. The clearest distinctions among these various types of currents are made in Table I of Ref. 21. Hiro currents arise "by instability acting as current generator," while Evans currents arise "by instability acting as voltage generator." That is, they are two limits of the same phenomenon. The current generator limit arises when these currents are driven at whatever level is required to slow the growth of the instability. Evans currents arise when these currents are too weak to be significant because the plasma equilibrium is more efficiently preserved by some other effect such as induced currents in the walls. Both Hiro and Evans currents are "Highly concentrated at the plasma edge."

Table I of Ref. 21 states halo currents arise from "Questionable use of equilibrium reconstruction. No strong reason for existence." Table I also states halo currents are "Assumed to be driven by residual voltage outside the last closed magnetic surface. Diffused in space with open field lines." It is noted that halo currents are "Limited by the ion saturation current." No similar saturation is noted for Hiro and Evans currents.

In an earlier paper,[22] Zakharov gave more details about Hiro currents, which raise a number of physics issues. First, he discussed surface currents in the plasma edge, which are sometimes described as delta-function currents: "When the plasma column, which initially is in MHD equilibrium, is deformed, it requires special external fields to maintain the equilibrium. Without them, the surface currents would be excited at the plasma edge in order to eliminate the normal component of magnetic field to the plasma boundary." As noted in the Introduction, an external magnetic field is required to support a plasma equilibrium. The required currents can in principle be anywhere outside the surface—not just in a delta-function on the plasma surface. For example, in a resistive wall mode the currents required to support the kinked plasma state are in the surrounding walls. Zakharov further stated: "after touching the wall, the surface currents

at the plasma boundary will be shared with the wall in the form of negative Hiro currents regardless the gaps in the wall. This creates a new regime for MHD instabilities called the wall touching kink mode." Zakharov's statement has confusing aspects: (1) Tokamak plasmas are generally in contact with the chamber walls throughout their evolution. The poloidal magnetic field is not tangential to the chamber walls due to the vertical magnetic field required for tokamak equilibria. (2) As discussed in the Introduction, when a surface current on a kinked surface touches a wall it does so only at discreet points, which makes it difficult to understand why gaps in the wall are irrelevant.

The concept of a delta-function surface current raises several physics issues. (1) A delta-function current is not physically realizable since it requires an infinite density of charge carriers. (2) A delta-function current must flow along the magnetic field lines for otherwise an infinite force per unit volume would be required to balance $\vec{j} \times \vec{B}$. (3) When a current flows along the magnetic field lines in a region with magnetic surfaces then the current density has two qualitatively different patterns depending on whether the safety factor q on the magnetic surface is a low order rational number or not. When q is a rational number the current density flows in a helical pattern defined by that rational number, which means the current pattern does not have the flexibility of flow pattern needed to produce the required external magnetic field to support the perturbed equilibrium. In standard tokamaks, the external field required to support the least stable $n = 1$ kink is highly concentrated in a lobe on the low-field side of the plasma.[23] When q is poorly approximated by low order rational numbers, the current is essentially uniformly spread over the surface and the primary effects are to cause a jump in q and to change the external poloidal magnetic flux. Said differently, a sudden change in the external poloidal flux induces a current on the surface of an ideal plasma.

[1]ITER Physics Expert Group on Disruptions, Plasma Control, and MHD and ITER Physics Basis Editors, Nucl. Fusion **39**, 2251 (1999).
[2]T. C. Hender, J. C. Wesley, J. Bialek, A. Bondeson, A. H. Boozer, R. J. Buttery, A. Garofalo, T. P. Goodman, R. S. Granetz, Y. Gribov, O. Gruber, M. Gryaznevich, G. Giruzzi, S. Gunter, N. Hayashi, P. Helander, C. C. Hegna, D. F. Howell, D. A. Humphreys, G. T. A. Huysmans, A. W. Hyatt, A. Isayama, S. C. Jardin, Y. Kawano, A. Kellman, C. Kessel, H. R. Koslowski, R. J. La Haye, E. Lazzaro, Y. Q. Liu, V. Lukash, J. Manickam, S. Medvedev, V. Mertens, S. V. Mirnov, Y. Nakamura, G. Navratil, M. Okabayashi, T. Ozeki, R. Paccagnella, G. Pautasso, F. Porcelli, V. D. Pustovitov, V. Riccardo, M. Sato, O. Sauter, M. J. Schaffer, M. Shimada, P. Sonato, E. J. Strait, M. Sugihara, M. Takechi, A. D. Turnbull, E. Westerhof, D. G. Whyte, R. Yoshino, H. Zohm, and the ITPA MHD, Disruption and Magnetic Control Topical Group, Nucl. Fusion **47**, S128–S202 (2007).
[3]N. W. Eidietis, S. P. Gerhardt, R. S. Granetz, Y. Kawano, M. Lehnen, J. B. Lister, G. Pautasso, V. Riccardo, R. L. Tanna, A. J. Thornton, and The ITPA Disruption Database Participants, Nucl. Fusion **55**, 063030 (2015).
[4]O. Gruber, K. Lackner, G. Pautasso, U. Seidel, and B. Streibel, Plasma Phys. Controlled Fusion **35**, B191 (1993).
[5]L. E. Zakharov, Phys. Plasmas **15**, 062507 (2008).
[6]A. H. Boozer, Phys. Plasmas **19**, 058101 (2012).
[7]A. H. Boozer, Phys. Plasmas **20**, 082510 (2013).
[8]A. H. Boozer, Nucl. Fusion **55**, 025001 (2015).
[9]R. Fitzpatrick, Nucl. Fusion **51**, 053007 (2011).
[10]J. Manikam, A. Boozer, and S. Gerhardt, Phys. Plasmas **19**, 082103 (2012).
[11]P. Noll, P. Andrew, M. Buzio, R. Litunovsky, T. Raimondi, V. Riccardo, and M. Verrecchia, *Fusion Technology* 1996, edited by C. Varandas and F. Serra (Elsevier, Amsterdam 1997), Vol. I, p. 751.
[12]V. D. Shafranov and L. Zakharov, Nucl. Fusion **12**, 599 (1972).
[13]A. H. Boozer, Phys. Plasmas **19**, 052508 (2012).
[14]V. Riccardo, G. Arnoux, P. Cahyna, T. C. Hender, A. Huber, S. Jachmich, V. Kiptily, R. Koslowski, L. Krlin, M. Lehnen, A. Loarte, E. Nardon, R. Paprok, D. Tskhakaya (Sr.), and JET-EFDA contributors, Plasma Phys. Controlled Fusion **52**, 124018 (2010).
[15]G. Pautasso, L. Giannone, O. Gruber, A. Herrmann, M. Maraschek, K. H. Schuhbeck, and the ASDEX Upgrade Team, Nucl. Fusion **51**, 043010 (2011).
[16]S. P. Gerhardt, Nucl. Fusion **53**, 023005 (2013).
[17]J. Bialek, A. H. Boozer, M. E. Mauel, and G. A. Navratil, Phys. Plasmas **8**, 2170 (2001).
[18]J.-K. Park, A. H. Boozer, and A. H. Glasser, Phys. Plasmas **14**, 052110 (2007).
[19]D. Bohm, "Minimum ionic kinetic energy for a stable sheath," in *The Characteristics of Electrical Discharges in Magnetic Fields*, edited by A. Guthrie and R. K. Wakerling (McGraw-Hill, New York, 1949), p. 77.
[20]A. H. Boozer, Plasma Phys. Controlled Fusion **52**, 124002 (2010).
[21]L. E. Zakharov, S. A. Galkin, S. N. Gerasimov, and JET-EFDA Contributors, Phys. Plasmas **19**, 055703 (2012).
[22]L. E. Zakharov, Phys. Plasmas **18**, 062503 (2011).
[23]J. K. Park, M. J. Schaffer, J. E. Menard, and A. H. Boozer, Phys. Rev. Lett. **99**, 195003 (2007).
[24]S. Gerhardt, private communication (2014).